Evaluation of the two-photon exchange graphs for the $2p_{1/2}$-$2s$ transition in Li-like ions

V. A. Yerokhin,[1,2] A. N. Artemyev,[3] V. M. Shabaev,[1,2] M. M. Sysak,[2] O. M. Zherebtsov,[2] and G. Soff[4]

[1]*Max-Planck-Institut für Physik Komplexer Systeme, Nöthnitzer Straße 38, D-01187 Dresden, Germany*

[2]*Department of Physics, St. Petersburg State University, Oulianovskaya 1, Petrodvorets, St. Petersburg 198904, Russia*

[3]*Centro de Química, Instituto Venezolano de Investigaciones Científicas, IVIC, Apartado 21827, Caracas 1020-A, Venezuela*

[4]*Institut für Theoretische Physik, TU Dresden, Mommsenstraße 13, D-01062 Dresden, Germany*

We present *ab initio* calculations of the complete gauge invariant set of the two-photon exchange graphs for the $2p_{1/2}$-$2s$ transition energy in Li-like high-Z ions. The evaluation is carried out to all orders in $Z\alpha$ in the range $Z = 20$–100. Results are compared with calculations based on relativistic many-body perturbation theory. All presently available contributions to the $2p_{1/2}$-$2s$ transition energy are collected. The resulting theoretical predictions are compared with experimental data.

I. INTRODUCTION

Heavy few-electron atoms provide an excellent possibility for testing quantum electrodynamics (QED) in the strong Coulomb field of the nucleus. Considerable progress in experimental investigations of these systems has stimulated theorists to evaluate the complete set of radiative corrections in second order in the fine structure constant α. Since the nuclear field is strong, consideration should be given to all orders in the coupling constant $Z\alpha$. The Lamb-shift calculation, complete to order α^2, still remains one of the challenging theoretical problems. Up to now, such a calculation has been carried out only for the two-electron contribution to the ground-state Lamb shift in He-like ions, which can be measured directly by comparing ionization energies of He-like and H-like ions [1,2]. Two-photon exchange corrections for these systems were calculated by Blundell *et al.* [3] and by Lindgren and co-workers [4]. The corresponding self-energy and vacuum-polarization screening diagrams were evaluated in our investigations [5,6] and by Persson and co-workers [7,8]. An analogous calculation for excited states of He-like ions is still under way. In Ref. [9], we evaluated the vacuum-polarization screening correction for low-lying excited states of He-like high-Z ions. For nonmixed states, the corresponding two-photon exchange correction was calculated recently by Mohr and Sapirstein [10].

While He-like systems are of experimental interest, the best experimental precision is achieved for $2p$-$2s$ transitions in Li-like ions [11–16]. In our previous investigations [17,18] we calculated the two-electron self-energy and vacuum-polarization corrections for the $2p_{1/2}$-$2s$ transition in Li-like high-Z ions. In this paper we report on the evaluation of the last unknown two-electron contribution of order α^2 for the transition under consideration, the two-photon exchange correction. The corresponding calculation was presented recently for some high-Z ions in Ref. [19]. In the present investigation we evaluate the two-photon exchange correction for a wide interval of the nuclear charge numbers Z and give a detailed description of the calculation procedure.

The plan of the paper is as follows. In the next section we derive basic formulas for the energy shift arising from the two-photon exchange of the valence electron with the $(1s)^2$

shell in high-Z Li-like ions. In Sec. III we discuss some details of the numerical evaluation. Section IV presents the numerical results and their comparison with the approximate treatment based on the Breit approximation. In the last section we collect all presently available contributions to the $2p_{1/2}$-$2s$ transition energy in high-Z Li-like ions and compare theoretical predictions with available experimental data.

Relativistic units are used in this article ($\hbar = c = 1$).

II. DERIVATION OF GENERAL FORMULAS

Our derivation of formulas is based on the two-time Green function (TTGF) method developed by Shabaev [20,21]. Here we present only a few basic formulas of the formalism which we will need in our derivation. For a detailed description of the method we refer to the recent review [22]. The starting point of the TTGF method is the standard N-particle Green function in the mixed energy-coordinate representation $G(q'_1, \ldots, q'_N; q_1, \ldots, q_N)$, where $q_i \equiv (p_i^0, \mathbf{x}_i)$. The Feynman rules for the Green function in the mixed representation can be found in Refs. [21,22]. Now we introduce the so-called *two-time* Green function

$$
g(E, \mathbf{x}'_1, \ldots, \mathbf{x}'_N; \mathbf{x}_1, \ldots, \mathbf{x}_N) \delta(E - E')
$$
$$
= \frac{2\pi}{i} \frac{1}{N!} \int_{-\infty}^{\infty} dp_1^0 \cdots dp_N^0 \, dp'_1^0 \cdots dp'_N^0
$$
$$
\times \delta(E - p_1^0 - \cdots - p_N^0) \delta(E' - p'_1^0 - \cdots - p'_N^0)
$$
$$
\times G(q'_1, \ldots, q'_N; q_1, \ldots, q_N) \gamma_1^0 \cdots \gamma_N^0. \quad (1)
$$

Here, we integrate over all relative energies of incoming and outgoing electrons and add the physical condition of the conservation of the total energy. In the time representation this corresponds to the alignment of the relative time of the incoming and outgoing electrons, respectively. An important statement is that $g(E)$ contains the full information about the energy levels of the system.

Consider now how to extract the energy of a single level k of an N-electron system from $g(E)$. We are interested in the energy shift $\Delta E_k = E_k - E_k^{(0)}$ caused by the interaction with the quantized electromagnetic field. Here, the unper-
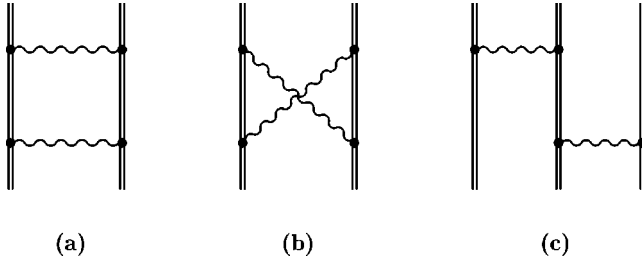
FIG. 1. The two-photon exchange diagrams.

turbed energy $E_k^{(0)}$ is the sum of the one-electron Dirac energies, $E_k^{(0)} = \varepsilon_1 + \varepsilon_2 + \cdots + \varepsilon_N$. The energy shift of an isolated level k is given by

$$\Delta E_k = \frac{(2\pi i)^{-1} \oint_\Gamma dE\, \Delta E\, \Delta g_{kk}(E)}{1 + (2\pi i)^{-1} \oint_\Gamma dE\, \Delta g_{kk}(E)}, \qquad (2)$$

where the contour Γ surrounds only the unperturbed level $E = E_k^{(0)}$ and is oriented counterclockwise, $\Delta E = E - E_k^{(0)}$, $\Delta g_{kk}(E) = g_{kk}(E) - g_{kk}^{(0)}(E)$, $g_{kk}(E) = \langle u_k | g(E) | u_k \rangle$, u_k is the unperturbed wave function, and $g_{kk}^{(0)}(E) = (E - E_k^{(0)})^{-1}$ is the function $g_{kk}(E)$ in the zeroth-order approximation. By expanding both the numerator and the denominator in Eq. (2) in the standard power series in α, energy corrections of different orders are obtained. We write the α expansion of the Green function $g(E)$ as

$$g(E) = g^{(0)}(E) + g^{(1)}(E) + g^{(2)}(E) + \cdots, \qquad (3)$$

where the superscript indicates the order in α. For the second-order correction we have

$$\Delta E_k^{(2)} = \frac{1}{2\pi i} \oint_\Gamma dE\, \Delta E\, \Delta g_{kk}^{(2)}(E)$$

$$- \frac{1}{2\pi i} \oint_\Gamma dE\, \Delta E\, \Delta g_{kk}^{(1)}(E) \frac{1}{2\pi i} \oint_\Gamma dE'\, \Delta g_{kk}^{(1)}(E'). \qquad (4)$$

In the present investigation we are interested in the two-photon exchange corrections. The corresponding Feynman diagrams for $\Delta g^{(2)}(E)$ are presented in Fig. 1. We refer to the diagram in Fig. 1(c) as the *three-electron* correction and to the diagrams in Figs. 1(a) and 1(b) as the *ladder* and the *crossed* contribution, respectively. A detailed analysis of the two-photon exchange diagrams was presented by Shabaev and Fokeeva [23] for the case of the one-determinant two-electron wave function. Here we generalize that derivation for the three-electron states with one electron outside the $(1s)^2$ shell. In our case the unperturbed wave function u_k is

$$u_k = \frac{1}{\sqrt{3!}} \sum_P (-1)^P \psi_{Pa}(\mathbf{x}_1) \psi_{Pb}(\mathbf{x}_2) \psi_{Pv}(\mathbf{x}_3), \qquad (5)$$

where v denotes the valence electron, a and b are the electrons in the $(1s)^2$ shell, and P is the permutation operator.

For brevity, we will use the following notations in what follows: $I(\omega) = e^2 \alpha^\mu \alpha^\nu D_{\mu\nu}(\omega)$, $I_{abcd}(\omega) = \langle ab | I(\omega) | cd \rangle$, $I_{ab;cd} = I_{abcd}(\Delta_{bd}) - I_{bacd}(\Delta_{ad})$, $I_{ab;cd}(p) = I_{abcd}(\Delta_{bd} + p) - I_{bacd}(\Delta_{ad} + p)$, $\tilde{I}_{ab;cd} = I_{abcd}(\Delta_{ca}) - I_{abdc}(\Delta_{da})$, and $I'(\omega) = dI(\omega)/d\omega$. Here, $\Delta_{ab} = \varepsilon_a - \varepsilon_b$, $\alpha^\mu = (1, \boldsymbol{\alpha})$ are the Dirac matrices, and $D_{\mu\nu}(\omega)$ is the photon propagator. For simplicity, we restrict our present consideration only to the Feynman and the Coulomb gauges. In this case the following symmetry properties of the operator I are valid: $I(\omega) = I(-\omega)$, $I'(0) = 0$, and $I_{abcd}(\omega) = I_{badc}(\omega)$. We note also that the operator I preserves the total angular momentum projection, i.e., the condition $\mu_a + \mu_b = \mu_c + \mu_d$ is valid for the nonvanishing matrix element $I_{abcd}(\omega)$, where μ denotes the angular-momentum projection of the corresponding electron.

A. Three-electron contribution

First we discuss the three-electron correction. It can be represented by the diagram shown in Fig. 1(c), assuming that all possible permutations over the incoming and the outgoing electrons are accounted for. The Feynman rules [21,22] yield

$$\Delta g_{kk}^{(2)}(E) = \sum_{PQ} (-1)^{P+Q} \sum_n \left(\frac{i}{2\pi}\right)^4 \int dp_1\, dp_2\, dp_1'\, dp_2'$$

$$\times \frac{1}{(p_1' - u\varepsilon_{P1})(p_2' - u\varepsilon_{P2})(E - p_1' - p_2' - u\varepsilon_{P3})}$$

$$\times \frac{1}{(p_1 - u\varepsilon_{Q1})(p_2 - u\varepsilon_{Q2})(E - p_1 - p_2 - u\varepsilon_{Q3})}$$

$$\times \frac{I_{P2P3nQ3}(p_1 + p_2 - p_1' - p_2') I_{P1nQ1Q2}(p_1 - p_1')}{p_1 + p_2 - p_1' - u\varepsilon_n}, \qquad (6)$$

where $u = 1 - i0$, and P and Q are the permutation operators acting on the outgoing and the incoming electrons, respectively. All integrations here and in what follows are assumed to extend over the interval $(-\infty, \infty)$, if not stated otherwise. The integration variables p_i in Eq. (6) correspond to p_i^0 in Eq. (1). For brevity, the index of the zeroth component is omitted here and in what follows. We divide the function $\Delta g_{kk}^{(2)}$ into two portions $\Delta g_{ir}^{(2)}$ and $\Delta g_{red}^{(2)}$ that correspond to the irreducible and the reducible parts of the correction, respectively. The reducible part is defined as the contribution in which the energy of the intermediate three-electron state coincides with the energy of the initial state of the atom. The irreducible part is the remainder. The expression for $\Delta g_{red}^{(2)}$ is given by Eq. (6) where the summation over n is restricted by the condition $\varepsilon_n = \varepsilon_{Q1} + \varepsilon_{Q2} - \varepsilon_{P1}$, and $\Delta g_{ir}^{(2)}$ is the remaining contribution.

1. Irreducible part

Now we consider the part of the first term in Eq. (4) that originates from the irreducible three-electron contribution

$$\Delta E_{\mathrm{ir}}^{3\mathrm{el}} = \frac{1}{2\pi i} \oint_{\Gamma} dE\, \Delta E\, \Delta g_{\mathrm{ir}}^{(2)}(E). \qquad (7)$$

While the derivation in this case is relatively simple, we describe it in detail in order to illustrate the technique, which will be directly applied to other contributions.

From Eq. (7) it is clear that only a part of $\Delta g_{\mathrm{ir}}^{(2)}$ with a singularity of order $1/(\Delta E)^2$ or higher yields a nonvanishing contribution to $\Delta E_{\mathrm{ir}}^{3\mathrm{el}}$. Therefore, we can rearrange the original expression, dropping out less singular terms. As an illustration, we consider a typical contribution to $\Delta g_{\mathrm{ir}}^{(2)}$ written in the compact form

$$\Delta g(E) = \left(\frac{i}{2\pi}\right)^2 \int dp_1\, dp_2 \frac{F(p_1,p_2)}{(p_1-\varepsilon_1+i0)(p_2-\varepsilon_2+i0)(E-p_1-p_2-\varepsilon_3+i0)}. \qquad (8)$$

Application of the identity

$$\frac{1}{x+i0} = \frac{2\pi}{i}\delta(x) + \frac{1}{x-i0} \qquad (9)$$

to the factor $1/(p_1-\varepsilon_1+i0)$ yields

$$\Delta g(E) = \frac{i}{2\pi} \int dp_2 \frac{F(\varepsilon_1,p_2)}{(p_2-\varepsilon_2+i0)(E-\varepsilon_1-p_2-\varepsilon_3+i0)}$$

$$+ \left(\frac{i}{2\pi}\right)^2 \int dp_1\, dp_2 \frac{F(p_1,p_2)}{(p_1-\varepsilon_1-i0)(p_2-\varepsilon_2+i0)(E-p_1-p_2-\varepsilon_3+i0)}. \qquad (10)$$

Here, the first term possesses an additional singularity at $E=E_k^{(0)}\equiv\varepsilon_1+\varepsilon_2+\varepsilon_3$ as compared to the second term. To prove this, we note that in the first term the contour of the p_2 integration is squeezed between two poles $p_2=\varepsilon_2\pm i0$ in the limit $E=E_k^{(0)}$. This means that a singularity appears at $E=E_k^{(0)}$ after the integration over p_2 is carried out. The singular factor can be explicitly separated by using the identity

$$\frac{1}{(p_2-\varepsilon_2+i0)(E-\varepsilon_1-p_2-\varepsilon_3+i0)} = \frac{1}{\Delta E}\left(\frac{1}{p_2-\varepsilon_2+i0} + \frac{1}{E-\varepsilon_1-p_2-\varepsilon_3+i0}\right), \qquad (11)$$

where the expression in the parentheses yields a regular function of E inside Γ after the integration over p_2 is carried out. In the second term of Eq. (10) both poles of the p_1 integration are in the same complex half plane, and we can shift the integration contour away from the poles. This shows that the integrations over p_1 and p_2 do not create any singularities at $E=E_k^{(0)}$ in this case.

In order to separate the contribution of order $1/(\Delta E)^2$ from $\Delta g_{\mathrm{ir}}^{(2)}$, we apply the identities (9) and (11) twice. This yields

$$\Delta g_{\mathrm{ir}}^{(2)}(E) = \frac{1}{(\Delta E)^2} \sum_{PQ} (-1)^{P+Q} \sum_{\varepsilon_n \neq \varepsilon_{Q1}+\varepsilon_{Q2}-\varepsilon_{P1}} \left(\frac{i}{2\pi}\right)^2 \int dp_2\, dp_2' \left(\frac{1}{p_2'-u\varepsilon_{P2}} + \frac{1}{E-\varepsilon_{P1}-p_2'-u\varepsilon_{P3}}\right)$$

$$\times \left(\frac{1}{p_2-u\varepsilon_{Q2}} + \frac{1}{E-\varepsilon_{Q1}-p_2-u\varepsilon_{Q3}}\right) \frac{I_{P2P3nQ3}(\varepsilon_{Q1}+p_2-\varepsilon_{P1}-p_2')I_{P1nQ1Q2}(\Delta_{Q1P1})}{\varepsilon_{Q1}+p_2-\varepsilon_{P1}-u\varepsilon_n} + (\text{less singular terms}).$$

$$(12)$$

Now the integration over E in Eq. (7) can be easily performed. After that, the integrations over p_2 and p_2' are carried out by employing the identity

$$\frac{1}{p_2 - \varepsilon_{Q2} + i0} + \frac{1}{-p_2 + \varepsilon_{Q2} + i0} = \frac{2\pi}{i} \delta(p_2 - \varepsilon_{Q2}). \tag{13}$$

The final expression for the irreducible part of the three-electron contribution is

$$\Delta E_{\mathrm{ir}}^{3\mathrm{el}} = \sum_{PQ} (-1)^{P+Q}$$

$$\times \sum_n{}' \frac{I_{P2P3nQ3}(\Delta_{P3Q3}) I_{P1nQ1Q2}(\Delta_{Q1P1})}{\varepsilon_{Q1} + \varepsilon_{Q2} - \varepsilon_{P1} - \varepsilon_n}, \tag{14}$$

where the prime on the sum indicates that terms with vanishing denominator should be omitted in the summation.

While just this expression can be used for the numerical evaluation, it will look more transparent if we write the triple permutations explicitly:

$$\Delta E_{\mathrm{ir}}^{3\mathrm{el}} = \sum_n{}' \left\{ \frac{I_{23;n3}\tilde{I}_{1n;12}}{\varepsilon_2 - \varepsilon_n} - \frac{I_{23;n2}\tilde{I}_{1n;13}}{\varepsilon_3 - \varepsilon_n} + \frac{I_{23;n1}\tilde{I}_{1n;23}}{\varepsilon_2 + \varepsilon_3 - \varepsilon_1 - \varepsilon_n} \right.$$

$$- \frac{I_{13;n3}\tilde{I}_{2n;12}}{\varepsilon_1 - \varepsilon_n} + \frac{I_{13;n2}\tilde{I}_{2n;13}}{\varepsilon_1 + \varepsilon_3 - \varepsilon_2 - \varepsilon_n} - \frac{I_{13;n1}\tilde{I}_{2n;23}}{\varepsilon_3 - \varepsilon_n}$$

$$\left. + \frac{I_{12;n3}\tilde{I}_{3n;12}}{\varepsilon_1 + \varepsilon_2 - \varepsilon_3 - \varepsilon_n} - \frac{I_{12;n2}\tilde{I}_{3n;13}}{\varepsilon_1 - \varepsilon_n} + \frac{I_{12;n1}\tilde{I}_{3n;23}}{\varepsilon_2 - \varepsilon_n} \right\}, \tag{15}$$

where $I_{ab;cd} = I_{abcd}(\Delta_{bd}) - I_{bacd}(\Delta_{ad})$ and $\tilde{I}_{ab;cd} = I_{abcd}(\Delta_{ca}) - I_{abdc}(\Delta_{da})$.

2. Reducible part

The expression for $\Delta g_{\mathrm{red}}^{(2)}$ reads

$$\Delta g_{\mathrm{red}}^{(2)}(E) = \sum_{PQ} (-1)^{P+Q} \sum_{\varepsilon_n = \varepsilon_{Q1} + \varepsilon_{Q2} - \varepsilon_{P1}} \left(\frac{i}{2\pi}\right)^4 \int dp_1\, dp_2\, dp_1'\, dp_2' \frac{1}{(p_1' - u\varepsilon_{P1})(p_2' - u\varepsilon_{P2})(E - p_1' - p_2' - u\varepsilon_{P3})}$$

$$\times \frac{1}{(p_1 - u\varepsilon_{Q1})(p_2 - u\varepsilon_{Q2})(E - p_1 - p_2 - u\varepsilon_{Q3})} \frac{I_{P2P3nQ3}(p_1 + p_2 - p_1' - p_2') I_{P1nQ1Q2}(p_1 - p_1')}{p_1 + p_2 - p_1' - \varepsilon_{Q1} - \varepsilon_{Q2} + \varepsilon_{P1} + i0}. \tag{16}$$

We rewrite this expression keeping terms with the singularity of order $1/(\Delta E)^2$ and higher, analogously to that for the irreducible part. Applying identity (9) to the factors $1/(p_1' - u\varepsilon_{P1})$ and $1/(E - p_1 - p_2 - u\varepsilon_{Q3})$, we obtain

$$\Delta g_{\mathrm{red}}^{(2)}(E) = \frac{1}{\Delta E} \sum_{PQ} (-1)^{P+Q} \sum_{\varepsilon_n = \varepsilon_{Q1} + \varepsilon_{Q2} - \varepsilon_{P1}} \left(\frac{i}{2\pi}\right)^2 \int dp_2\, dp_2' \frac{I_{P2P3nQ3}(E - \varepsilon_{Q3} - \varepsilon_{P1} - p_2')}{(p_2' - u\varepsilon_{P2})(E - \varepsilon_{P1} - p_2' - u\varepsilon_{P3})}$$

$$\times \frac{I_{P1nQ1Q2}(E - \varepsilon_{Q3} - \varepsilon_{P1} - p_2)}{(E - p_2 - \varepsilon_{Q3} - u\varepsilon_{Q1})(p_2 - u\varepsilon_{Q2})} + (\text{terms with a singularity of order } 1/\Delta E \text{ or lower}). \tag{17}$$

Next, we use Eq. (11) to separate factors $1/\Delta E$ explicitly and perform the energy integration. The resulting expression is divided into two parts,

$$\frac{1}{2\pi i} \oint_\Gamma dE\, \Delta E\, \Delta g_{\mathrm{red}}^{(2)}(E) = \Delta E_{\mathrm{red}}^{3\mathrm{el}} + \Delta \tilde{E}_{\mathrm{red}}^{3\mathrm{el}}, \tag{18}$$

where

$$\Delta E_{\mathrm{red}}^{3\mathrm{el}} = \frac{1}{2} \sum_{PQ} (-1)^{P+Q} \sum_{\varepsilon_n = \varepsilon_{Q1} + \varepsilon_{Q2} - \varepsilon_{P1}} [I'_{P2P3nQ3}(\Delta_{P3Q3}) I_{P1nQ1Q2}(\Delta_{Q1P1}) + I_{P2P3nQ3}(\Delta_{P3Q3}) I'_{P1nQ1Q2}(\Delta_{Q1P1})], \tag{19}$$

$$\Delta \tilde{E}_{\mathrm{red}}^{3\mathrm{el}} = -\frac{1}{2} \sum_{PQ} (-1)^{P+Q} \sum_{\varepsilon_n = \varepsilon_{Q1} + \varepsilon_{Q2} - \varepsilon_{P1}} \frac{i}{2\pi} \int dp\, \frac{1}{(p + i0)^2}$$

$$\times \{[I_{P2P3nQ3}(\Delta_{P3Q3} + p) + I_{P2P3nQ3}(\Delta_{P3Q3} - p)] I_{P1nQ1Q2}(\Delta_{Q1P1}) + I_{P2P3nQ3}(\Delta_{P3Q3})$$

$$\times [I_{P1nQ1Q2}(\Delta_{Q1P1} + p) + I_{P1nQ1Q2}(\Delta_{Q1P1} - p)]\}. \tag{20}$$

We will show below that $\Delta E^{3\mathrm{el}}_{\mathrm{red}}$ yields the total reducible three-electron contribution, while $\Delta \widetilde{E}^{3\mathrm{el}}_{\mathrm{red}}$ is completely cancelled when considered together with the second term in Eq. (4) (the *disconnected* contribution) and with the reducible part of the two-electron contribution. To see this, we should write the sum over n and permutations P,Q in Eqs. (19) and (20) explicitly. While the result looks rather cumbersome, its general structure can be understood from the expression for the irreducible part (15). Loosely speaking, the reducible part corresponds to the terms with vanishing denominator which are omitted in the n summation of Eq. (15). We note that the number of such terms is different in two cases, if all three electrons have different energies and in the case under consideration with two electrons of the same energy.

We will use the notations a and b for the electrons in the $(1s)^2$ shell, v for the valence ($2s$ or $2p_{1/2}$) electron, ε_c and ε_v for the energy of the core and the valence electron, respectively, and μ for the projection of the angular momentum. Writing the summation over n in Eqs. (19) and (20) explicitly, we note that the condition, e.g., $\varepsilon_n = \varepsilon_v$ involves two possibilities: $\mu_n = \mu_v$ (denoted as $n = v$) and $\mu_n = -\mu_v$ (denoted as $n = \bar{v}$). After simple but rather tedious manipulations, we express Eqs. (19) and (20) as follows (with $\Delta \widetilde{E}^{3\mathrm{el}}_{\mathrm{red}}$ divided into two parts, $\Delta \widetilde{E}^{3\mathrm{el}}_{\mathrm{red},1}$ and $\Delta \widetilde{E}^{3\mathrm{el}}_{\mathrm{red},2}$):

$$\Delta E^{3\mathrm{el}}_{\mathrm{red}} = \sum_{\mu_a} \left[I'_{vaav}(\Delta)(I_{ab;ab} - I_{bv;bv}) + \tfrac{1}{2} I'_{av\overline{va}}(\Delta) I_{\overline{av};av} \right.$$
$$\left. + \tfrac{1}{2} I'_{\overline{avv}a}(\Delta) I_{va;\overline{va}} \right], \tag{21}$$

$$\Delta \widetilde{E}^{3\mathrm{el}}_{\mathrm{red},1} = -\frac{i}{2\pi} \int dp \frac{1}{(p+i0)^2} \{[I_{bv;bv}(p) + I_{bv;bv}(-p)]$$
$$\times [I_{av;av} + I_{ab;ab}] + [I_{av;av}(p) + I_{av;av}(-p)]$$
$$\times [I_{bv;bv} + I_{ab;ab}] + [I_{ab;ab}(p) + I_{ab;ab}(-p)]$$
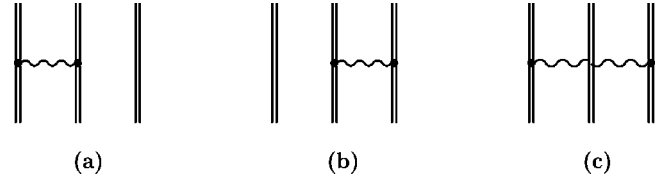$$\times [I_{av;av} + I_{bv;bv}] \}, \tag{22}$$

$$\Delta \widetilde{E}^{3\mathrm{el}}_{\mathrm{red},2} = \sum_{\mu_a} \frac{i}{4\pi} \int dp \frac{1}{(p+i0)^2}$$
$$\times \{[I_{va;\overline{va}}(p) + I_{va;\overline{va}}(-p)] I_{\overline{av};av}$$
$$+ I_{va;\overline{va}}[I_{\overline{av};av}(p) + I_{\overline{av};av}(-p)]\}, \tag{23}$$

where it is taken into account that the operator I preserves the total angular-momentum projection. Here, $I_{ab;cd} = I_{abcd}(\Delta_{bd}) - I_{bacd}(\Delta_{ad})$, $I_{ab;cd}(p) = I_{abcd}(\Delta_{bd} + p) - I_{bacd}(\Delta_{ad} + p)$, $\Delta = \varepsilon_v - \varepsilon_c$, $\mu_{\bar{v}} = -\mu_v$, and $\mu_{\bar{a}} = -\mu_a$. As we will show below, $\Delta \widetilde{E}^{3\mathrm{el}}_{\mathrm{red},1}$ and $\Delta \widetilde{E}^{3\mathrm{el}}_{\mathrm{red},2}$ are exactly canceled when considered together with the disconnected contribution [Eq. (31)] and the reducible part of the ladder contribution [Eq. (38)]. Therefore, $\Delta E^{3\mathrm{el}}_{\mathrm{red}}$ [Eq. (21)] yields the final expression for the reducible three-electron contribution.

B. Disconnected contribution

Now we consider the second term in Eq. (4), to which we refer as the *disconnected* contribution:

$$\Delta E^{\mathrm{disc}} = -\frac{1}{2\pi i} \oint_{\Gamma} dE \, \Delta E \, \Delta g^{(1)}_{kk}(E) \frac{1}{2\pi i} \oint_{\Gamma} dE' \, \Delta g^{(1)}_{kk}(E'). \tag{24}$$

The Feynman diagrams contributing to $\Delta g^{(1)}$ are presented in Fig. 2. According to the Feynman rules [21,22], we have for the diagram in Fig. 2(a)

FIG. 2. Feynman diagrams contributing to the disconnected term.

$$\Delta g^{(1),2a}_{kk}(E) = \sum_{P} (-1)^P \left(\frac{i}{2\pi}\right)^3 \int dp_1 \, dp'_1 \, dp_3 \frac{1}{p_3 - u\varepsilon_3} I_{P1P212}(p_1 - p'_1) \delta_{P3,3}$$
$$\times \frac{1}{(p'_1 - u\varepsilon_{P1})(E - p'_1 - p_3 - u\varepsilon_{P2})} \frac{1}{(p_1 - u\varepsilon_1)(E - p_1 - p_3 - u\varepsilon_2)}. \tag{25}$$

(We note that some care should be taken in simplifying the summation over the permutations of the initial and final states in this separate diagram since the operator $I_{P1P212} \delta_{P3,3}$ is not symmetric with respect to permutations of the electrons. However, the sum of all diagrams in Fig. 2 is symmetric, which justifies our derivation.) The p_3 integration in Eq. (25) can be carried out, enclosing the integration contour in the lower half plane. It yields

$$\Delta g^{(1),2a}_{kk}(E) = \sum_{P} (-1)^P \left(\frac{i}{2\pi}\right)^2 \int dp_1 \, dp'_1 \frac{1}{(p'_1 - \varepsilon_{P1} + i0)(\Delta E - p'_1 + \varepsilon_{P1} + i0)} \frac{I_{P1P212}(p_1 - p'_1)}{(p_1 - \varepsilon_1 + i0)(\Delta E - p_1 + \varepsilon_1 + i0)}, \tag{26}$$

where the operator P is assumed to permute only two electrons. Having in mind the E' integration in Eq. (24), we should keep all terms that are singular at $E=E_k^{(0)}$. Applying identity (9) to the factors $1/(p_1-u\varepsilon_1)$ and $1/(p_1'-u\varepsilon_{P1})$, we obtain

$$\Delta g_{kk}^{(1),2a}(E)=\frac{1}{\Delta E}\sum_P (-1)^P \frac{i}{2\pi}$$

$$\times\int dp \frac{1}{(p-i0)(\Delta E-p+i0)}$$

$$\times[I_{P1P212}(\Delta_{1P1}-p)+I_{P1P212}(\Delta_{1P1}+p)]$$

$$+\frac{1}{(\Delta E)^2}\sum_P (-1)^P I_{P1P212}(\Delta_{1P1})$$

$$+(\text{terms regular at } E=E_k^{(0)}). \qquad (27)$$

For the remaining diagrams in Fig. 2 we derive similar expressions. The integration over the energy is now trivial. It yields

$$\frac{1}{2\pi i}\oint_\Gamma dE\,\Delta E\,\Delta g_{kk}^{(1)}(E)=\sum_P (-1)^P[I_{P1P212}(\Delta_{1P1})$$

$$+I_{P2P323}(\Delta_{P33})$$

$$+I_{P1P313}(\Delta_{P33})], \qquad (28)$$

$$\frac{1}{2\pi i}\oint_\Gamma dE\,\Delta g_{kk}^{(1)}(E)$$

$$=\sum_P (-1)^P \frac{i}{2\pi}\int dp \frac{-1}{(p+i0)^2}$$

$$\times\{I_{P1P212}(\Delta_{1P1}-p)+I_{P1P212}(\Delta_{1P1}+p)$$

$$+I_{P2P323}(\Delta_{P33}-p)+I_{P2P323}(\Delta_{P33}+p)$$

$$+I_{P1P313}(\Delta_{P33}-p)+I_{P1P313}(\Delta_{P33}+p)\}. \qquad (29)$$

For ΔE^{disc} we have

$$\Delta E^{\text{disc}}=\frac{i}{2\pi}\int dp \frac{1}{(p+i0)^2}[I_{12;12}(p)+I_{12;12}(-p)$$

$$+I_{13;13}(p)+I_{13;13}(-p)+I_{23;23}(p)+I_{23;23}(-p)]$$

$$\times[I_{12;12}+I_{13;13}+I_{23;23}]. \qquad (30)$$

Finally, we rewrite this expression for the three-electron state under consideration, explicitly separating a part canceled by Eq. (22),

$$\Delta E^{\text{disc}}=-\Delta\widetilde{E}_{\text{red},1}^{3\text{el}}+\frac{i}{2\pi}\int dp \frac{1}{(p+i0)^2}\{[I_{bv;bv}(p)$$

$$+I_{bv;bv}(-p)]I_{bv;bv}$$

$$+[I_{av;av}(p)+I_{av;av}(-p)]I_{av;av}$$

$$+[I_{ab;ab}(p)+I_{ab;ab}(-p)]I_{ab;ab}\}. \qquad (31)$$

The rest of the disconnected contribution vanishes when considered together with the reducible part of the ladder contribution [Eq. (38) and an analogous term from the ladder diagram with both electrons from the $(1s)^2$ shell].

C. Two-electron contribution

Only two electrons are involved in the photon exchange in Figs. 1(a) and 1(b), and, therefore, the three-electron problem can be decomposed into three two-electron problems. The two-electron contribution with both electrons from the $(1s)^2$ shell is the same as for the ground state of a He-like ion. It was evaluated in Refs. [3,4] and does not affect the $2p_{1/2}$-$2s$ transition energy. We shall be concerned here with the remaining corrections in which one electron line corresponds to the valence electron and the other one to the core electron. The ladder contribution is naturally divided into the irreducible and reducible parts. The reducible part is defined as the contribution in which the energy of the intermediate two-electron state coincides with the energy of the initial state. The irreducible part is the remainder. Often it is convenient also to divide these contributions into the direct and the exchange parts according to the relative alignment of the ingoing and outcoming states.

1. Irreducible part

Expressions for the crossed contribution and for the irreducible part of the ladder contribution are essentially the same as in the case considered in Ref. [23]. We write the sum of these two terms as

$$\Delta E_{\text{ir}}^{2\text{el}}=\sum_{n_1 n_2}' \frac{i}{2\pi}\int d\omega\left\{\frac{F_{\text{lad,dir}}(\omega,n_1 n_2)}{(\varepsilon_c-\omega-u\varepsilon_{n_1})(\varepsilon_v+\omega-u\varepsilon_{n_2})}\right.$$

$$+\frac{F_{\text{lad,ex}}(\omega,n_1 n_2)}{(\varepsilon_v-\omega-u\varepsilon_{n_1})(\varepsilon_c+\omega-u\varepsilon_{n_2})}$$

$$+\frac{F_{\text{cr,dir}}(\omega,n_1 n_2)}{(\varepsilon_c-\omega-u\varepsilon_{n_1})(\varepsilon_v-\omega-u\varepsilon_{n_2})}$$

$$\left.+\frac{F_{\text{cr,ex}}(\omega,n_1 n_2)}{(\varepsilon_v-\omega-u\varepsilon_{n_1})(\varepsilon_v-\omega-u\varepsilon_{n_2})}\right\}, \qquad (32)$$

where

$$F_{\text{lad,dir}}(\omega,n_1 n_2)=\sum_{\mu_c\mu_1\mu_2}\langle cv|I(\omega)|n_1 n_2\rangle\langle n_1 n_2|I(\omega)|cv\rangle, \qquad (33)$$

$$-F_{\text{lad,ex}}(\omega,n_1 n_2)=\sum_{\mu_c\mu_1\mu_2}\langle vc|I(\omega)|n_1 n_2\rangle$$

$$\times\langle n_1 n_2|I(\omega-\Delta)|cv\rangle, \qquad (34)$$

$$F_{\text{cr,dir}}(\omega,n_1 n_2)=\sum_{\mu_c\mu_1\mu_2}\langle cn_2|I(\omega)|n_1 v\rangle\langle n_1 v|I(\omega)|cn_2\rangle, \qquad (35)$$

$$-F_{\text{cr,ex}}(\omega,n_1 n_2)=\sum_{\mu_c\mu_1\mu_2}\langle vn_2|I(\omega)|n_1 v\rangle$$

$$\times\langle n_1 c|I(\omega-\Delta)|cn_2\rangle. \qquad (36)$$

Here c and v denote the core and the valence electron, respectively; μ stands for the angular momentum projection, ε indicates the Dirac energy of the corresponding state, and $\Delta=\varepsilon_v-\varepsilon_c$. The prime on the sum indicates that some terms are omitted in the summation. In the first, we restrict the summation over n_1,n_2 to exclude states that contribute to the reducible part of the ladder diagram, $(\varepsilon_{n_1}\varepsilon_{n_2})=(\varepsilon_c\varepsilon_v),(\varepsilon_v\varepsilon_c)$. Next, we exclude terms with singular infrared behavior $(\varepsilon_{n_1}\varepsilon_{n_2})=(\varepsilon_c\varepsilon_v)$ from the direct crossed contribution and $(\varepsilon_{n_1}\varepsilon_{n_2})=(\varepsilon_c\varepsilon_c),(\varepsilon_v\varepsilon_v)$ from the exchange crossed part. Some care should be taken of the nearly degenerate Dirac states. In particular, the $2s$ and the $2p_{1/2}$ states are split only by the finite nuclear size effect. It is convenient to treat these states in the same way. This means that we understand the above condition $(\varepsilon_{n_1}\varepsilon_{n_2})=(\varepsilon_v\varepsilon_v)$ in the point-nucleus limit.

2. Reducible part

The reducible part of the ladder diagram is given by Eq. (47) of Ref. [23]. Rewriting this expression in our notation and introducing the summation over angular-momentum projections of the core electron, we have

$$\Delta E_{\text{red}}^{\text{lad}}=\sum_{\mu_c}\sum_{\varepsilon_{n_1}+\varepsilon_{n_2}=\varepsilon_v+\varepsilon_c}\frac{i}{4\pi}\int d\omega\frac{-1}{(\omega+i0)^2}$$

$$\times[I_{cv;n_1 n_2}(-\omega)I_{n_1 n_2 cv}(\Delta_{n_2 v}+\omega)$$

$$+I_{cv;n_1 n_2}(\omega)I_{n_1 n_2 cv}(\Delta_{n_2 v})$$

$$+I_{cv;n_1 n_2}I_{n_1 n_2 cv}(\Delta_{n_2 v}-\omega)$$

$$+\cdots+\{\omega\rightarrow-\omega\}+\cdots]. \qquad (37)$$

The sum over n_1,n_2 is restricted by the condition $(n_1 n_2)=(\tilde v\tilde c),(\tilde c\tilde v)$, where $\varepsilon_{\tilde v}=\varepsilon_v$, $\varepsilon_{\tilde c}=\varepsilon_c$, and $\mu_{\tilde v},\mu_{\tilde c}$ are arbitrary. Writing the sum over n_1,n_2 explicitly, we have

$$\Delta E_{\text{red}}^{\text{lad}}=\sum_{\mu_c\mu_{\tilde v}\mu_{\tilde c}}\frac{i}{4\pi}\int d\omega\frac{-1}{(\omega+i0)^2}\{I_{cv;\tilde c\tilde v}(\omega)I_{\tilde c\tilde v;cv}(\omega)$$

$$+I_{cv;\tilde c\tilde v}(-\omega)I_{\tilde c\tilde v;cv}(-\omega)$$

$$+I_{cv;\tilde c\tilde v}[I_{\tilde c\tilde v;cv}(\omega)+I_{\tilde c\tilde v;cv}(-\omega)]$$

$$+[I_{cv;\tilde c\tilde v}(\omega)+I_{cv;\tilde c\tilde v}(-\omega)]I_{\tilde c\tilde v;cv}\}. \qquad (38)$$

Taking into account that the operator I preserves the total angular-momentum projection, we see that the $\mu_{\tilde v}$ and $\mu_{\tilde c}$ summation consists of two terms, $(\mu_{\tilde v},\mu_{\tilde c})=(\mu_v,\mu_c)$ and $(-\mu_v,-\mu_c)$. When $(\mu_{\tilde v},\mu_{\tilde c})=(\mu_v,\mu_c)$, the last two terms of Eq. (38) are canceled by the corresponding contribution from the disconnected term [Eq. (31)]. For $(\mu_{\tilde v},\mu_{\tilde c})=(-\mu_v,-\mu_c)$, the last two terms of Eq. (38) vanish when considered together with $\Delta\widetilde E_{\text{red},2}^{\text{3el}}$ [Eq. (23)]. The remainder is

$$\Delta E_{\text{red,r}}^{\text{lad}}=\sum_{\mu_c\mu_{\tilde v}\mu_{\tilde c}}\frac{i}{4\pi}\int d\omega\frac{-1}{(\omega+i0)^2}[I_{cv;\tilde c\tilde v}(\omega)I_{\tilde c\tilde v;cv}(\omega)$$

$$+\cdots+\{\omega\rightarrow-\omega\}+\cdots]. \qquad (39)$$

For further evaluation it is convenient to rewrite this expression using the definitions (33) and (34)

$$\Delta E_{\text{red,r}}^{\text{lad}}=-\frac{i}{4\pi}\int d\omega\frac{1}{(\omega+i0)^2}[F_{\text{lad,dir}}(\omega,cv)$$

$$+F_{\text{lad,ex}}(\Delta-\omega,cv)+F_{\text{lad,dir}}(\omega-\Delta,vc)$$

$$+F_{\text{lad,ex}}(\omega,vc)+\cdots+\{\omega\rightarrow-\omega\}+\cdots]. \qquad (40)$$

Next, we add the terms excluded from the crossed part of Eq. (32). The resulting contribution we refer to as $\Delta E_{\text{red}}^{\text{2el}}$. It reads

$$\Delta E_{\text{red}}^{\text{2el}}=\frac{i}{4\pi}\int d\omega\frac{1}{(\omega+i0)^2}[2F_{\text{cr,dir}}(-\omega,cv)$$

$$+2F_{\text{cr,ex}}(-\omega+\Delta,cc)+2F_{\text{cr,ex}}(-\omega,vv)$$

$$+2F_{\text{cr,ex}}(-\omega+\Delta_{vs},ss)-2F_{\text{lad,dir}}(\omega,cv)$$

$$-F_{\text{lad,ex}}(\omega+\Delta,cv)-F_{\text{lad,ex}}(-\omega+\Delta,cv)$$

$$-F_{\text{lad,dir}}(\omega-\Delta,vc)-F_{\text{lad,dir}}(-\omega-\Delta,vc)$$

$$-F_{\text{lad,ex}}(\omega,vc)-F_{\text{lad,ex}}(-\omega,vc)], \qquad (41)$$

where s denotes the Dirac state separated only by the finite nuclear size effect from the valence state. It can be shown (see Ref. [23] for details) that $F_{\text{lad,dir}}(\omega,cv)$ and $F_{\text{cr,dir}}(-\omega,cv)$ cancel each other exactly, and that the remaining contribution is infrared finite if considered as a whole. Therefore, the resulting expression reads

$$\Delta E_{\text{red}}^{\text{2el}}=\frac{i}{4\pi}\int d\omega\frac{1}{(\omega+i0)^2}[2F_{\text{cr,ex}}(-\omega+\Delta,cc)$$

$$+2F_{\text{cr,ex}}(-\omega,vv)+2F_{\text{cr,ex}}(-\omega+\Delta_{vs},ss)$$

$$-F_{\text{lad,ex}}(\omega+\Delta,cv)-F_{\text{lad,ex}}(-\omega+\Delta,cv)$$

$$-F_{\text{lad,dir}}(\omega-\Delta,vc)-F_{\text{lad,dir}}(-\omega-\Delta,vc)$$

$$-F_{\text{lad,ex}}(\omega,vc)-F_{\text{lad,ex}}(-\omega,vc)]. \qquad (42)$$

The final result for the two-photon exchange correction corresponding to the interaction of the valence ($2s$ or $2p_{1/2}$) electron with the $(1s)^2$ shell is given by the sum of Eqs. (15), (21), (32), and (42).

We note that our formulas reproduce the second-order many-body perturbation theory (MBPT) result if we neglect the energy dependence of the photon propagator in the Coulomb gauge and introduce projectors on the positive-energy part of the spectrum. After these assumptions, all reducible contributions vanish, and the ω integration in the two-electron part is carried out using Cauchy's theorem. Now the

crossed contribution also vanishes, and the ladder part yields the total two-electron correction within the MBPT approximation:

$$\Delta E_{\rm MBPT}^{\rm 2el} = \sum_{\mu_c} \sum_{n_1 n_2}{}' \frac{I_{cv;n_1 n_2}(0) I_{n_1 n_2 cv}(0)}{\varepsilon_c + \varepsilon_v - \varepsilon_{n_1} - \varepsilon_{n_2}}, \qquad (43)$$

where the summation over n_1, n_2 is restricted by the conditions $\varepsilon_{n_1} + \varepsilon_{n_2} \neq \varepsilon_c + \varepsilon_v$, $\varepsilon_{n_1} > 0$, $\varepsilon_{n_2} > 0$, and the photon propagators in the Coulomb gauge are assumed. The three-electron contribution within the MBPT approximation can be directly obtained from Eq. (15).

III. NUMERICAL EVALUATION

In this section we discuss the numerical evaluation of the two-photon exchange correction. As the three-electron part of the correction is relatively simple, we concentrate on the calculation of two-electron contributions.

The two-photon exchange correction corresponding to the interaction of the valence $2s$ or $2p_{1/2}$ electron with the $(1s)^2$ shell is given by the sum of Eqs. (15), (21), (32), and (42). The summation over magnetic substates and the angular integration can be carried out using standard techniques. The resulting expressions are given in the Appendix. The summation over the whole spectrum of intermediate states is performed using the method of the B-spline basis set for the Dirac equation [24]. In actual calculations, the basis set typically contained 50 positive- and 50 negative-energy states per angular-momentum quantum number κ. The finite size of the nucleus is accounted for by using the spherical distribution of the nuclear charge. The infinite partial-wave summation is terminated typically at $|\kappa| = 10$. The remainder of the sum is estimated by polynomial fitting in $1/|\kappa|$.

The most problematic part of the numerical evaluation is the integration over the energy of the virtual photon ω. In order to avoid strong oscillations arising for large real values of ω, we perform a Wick rotation of the integration contour, following the treatment of Ref. [3]. Some care should be taken for the pole and cut structure of the integrand, which is essentially more elaborate than for the $(1s)^2$ case. We note that the analytic structure of the integrand in our case is exactly the same as for the lowest excited states of He-like ions, investigated recently by Mohr and Sapirstein [10]. While the particular choice of integration contours is slightly different here, the analysis given in that work can be fully applied in our case as well.

The two-electron contribution is conveniently divided into the direct and the exchange parts, which are treated separately. The poles and the branch cuts of the integrand for the direct part of the ladder and the crossed contribution are shown in Figs. 3 and 4, respectively. We rotate the integration contour in the complex ω plane from the real to the imaginary axis, separating pole contributions that arise from intermediate states n with $0 < \varepsilon_n \leq \varepsilon_v$. For the direct part, the only complication as compared to the $(1s)^2$ case consists in a different structure of the pole terms, and the evaluation is very similar to that for the ground state of He-like ions. In
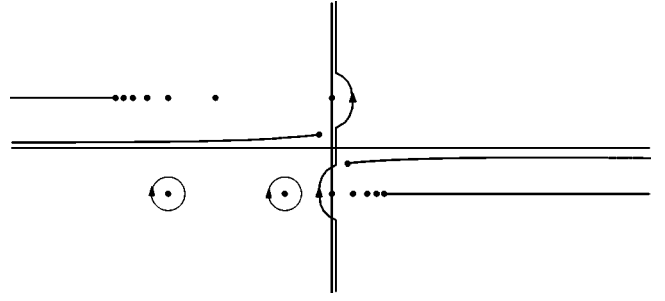

FIG. 3. The poles and the branch cuts of the integrand for the direct part of the ladder contribution, and the integration contour used for the evaluation of this correction.

the low-Z region, care is required for low values of ω because of poles of electron propagators encountered near the integration contour. This problem is handled by isolating terms with a near-singular behavior and employing a very dense grid for low values of ω. In order to calculate the direct part of the reducible contribution, we integrate by parts and perform a Wick rotation. This yields an expression that can be directly evaluated:

$$\Delta E_{\rm red}^{\rm 2el}({\rm dir}) = \frac{1}{2} [F_{\rm lad,dir}(\Delta, vc)]'$$

$$- \frac{1}{\pi} \int_0^\infty d\omega \frac{\omega}{\Delta^2 + \omega^2} \frac{d}{d\omega} F_{\rm lad,dir}(i\omega, vc),$$

$$(44)$$

where $F'(\Delta) = (dF(\omega)/d\omega)_{\omega=\Delta}$.

Let us consider the exchange parts of the ladder and the crossed contribution. Now the branch points of the photon propagators are shifted by $\Delta = \varepsilon_v - \varepsilon_c$ with respect to each other, as shown in Figs. 5 and 6. As a result, the integration contour is squeezed at two points $\omega = 0$ and $\omega = \Delta$. An additional complication arises from the presence of poles of electron propagators close to the "squeezed" part of the integration contour. The numerical evaluation of the exchange contribution is the most time consuming part of the calculation. In order to facilitate this, we divide the exchange contribution into two parts, the *irregular* part in which n_1 or n_2 corresponds to one of the $1s$, $2s$, $2p_{1/2}$ (and $2p_{3/2}$ for lower-
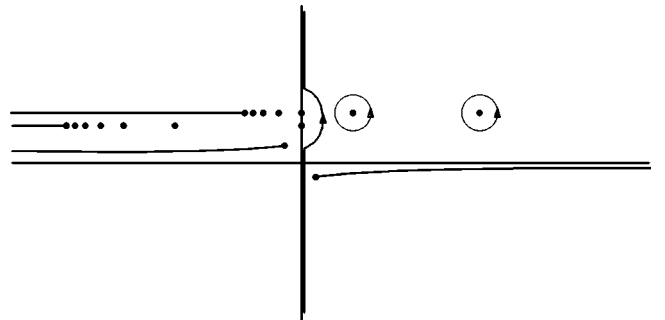

FIG. 4. The poles and the branch cuts of the integrand for the direct part of the crossed contribution, and the integration contour used for the evaluation of this correction.
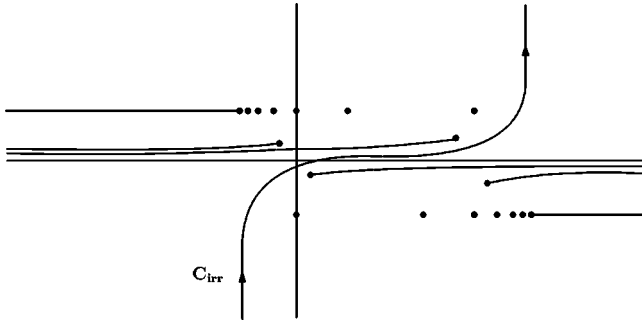
FIG. 5. The poles and the branch cuts of the integrand for the exchange part of the ladder contribution, and the integration contour C_{irr}.

Z atoms) states, and the *regular* part, the remainder. The regular part is the most numerically intensive one, but it does not contain any poles near the squeezed part of the integration contour. The calculation of the irregular part is more elaborate but less time consuming.

Evaluating the irregular part, we should keep the infinitesimal imaginary term $i0$ when a pole is encountered near the integration contour. In this case, the standard identity is used

$$\int_{\omega_1}^{\omega_2} d\omega \frac{f(\omega)}{\Delta_0 - \omega + i0} = P\int_{\omega_1}^{\omega_2} d\omega \frac{f(\omega)}{\Delta_0 - \omega} - i\pi f(\Delta_0) \tag{45}$$

($\Delta_0 \in [\omega_1, \omega_2]$), and the principal value of the integral is evaluated numerically. As can be seen from Fig. 6, two coinciding poles can be encountered near the integration contour in the exchanged crossed contribution. In this case, we rewrite the corresponding integral as

$$\int_{\omega_1}^{\omega_2} d\omega \frac{f(\omega)}{(\Delta_0 - \omega + i0)^2} = i\pi f'(\Delta_0) + \frac{f(\omega_2)}{\Delta_0 - \omega_2} - \frac{f(\omega_1)}{\Delta_0 - \omega_1}$$
$$- P\int_{\omega_1}^{\omega_2} d\omega \frac{f'(\omega)}{\Delta_0 - \omega}, \tag{46}$$
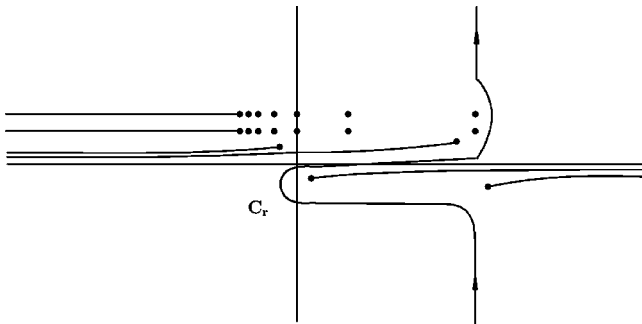
where $\Delta_0 \in [\omega_1, \omega_2]$.

FIG. 6. The poles and the branch cuts of the integrand for the exchange part of the crossed contribution, and the integration contour C_r.

For the numerical evaluation of the irregular and regular parts we employed two contours C_{irr} and C_r, which are shown in Figs. 5 and 6, respectively. While the choice of the contour is to some extent arbitrary, we use these two contours for the sake of convenience and in order to check the consistency of our numerical procedure. In our actual calculation the contour C_r was employed for the regular contribution, and C_{irr} for the irregular one. The contour C_{irr} can be divided into three parts: $[-\epsilon - i\infty, -\epsilon]$, $[-\epsilon, \Delta + \epsilon]$, and $[\Delta + \epsilon, \Delta + \epsilon + i\infty]$. Here, ϵ is a small positive constant which is introduced to allow for the numerical evaluation of the principal value of an integral with a singularity at the points $\omega = 0$ or $\omega = \Delta$. On the interval $[-\epsilon, \Delta + \epsilon]$ we carry out the ω integration of the irregular part before the summation over n_1 and n_2. In all other cases, the summation over the spectrum for a given angular-momentum quantum number is performed first.

The exchange part of the reducible contribution is calculated after integration by parts,

$$\Delta E_{\text{red}}^{2\text{el}}(\text{exch})$$

$$= -\frac{1}{2}[F_{\text{cr,ex}}(\Delta, cc) + F_{\text{cr,ex}}(0, vv) + F_{\text{cr,ex}}(\Delta_{vs}, ss)]'$$

$$+ \frac{i}{2\pi}P\int_{-\infty}^{\infty} \frac{d\omega}{\omega} \frac{d}{d\omega}[F_{\text{cr,ex}}(\Delta + \omega, cc) + F_{\text{cr,ex}}(\omega, vv)$$

$$+ F_{\text{cr,ex}}(\Delta_{vs} + \omega, ss) - 2F_{\text{lad,ex}}(\omega, vc)]. \tag{47}$$

In our implementation the principal value of the integral in Eq. (47) is evaluated as follows:

$$\frac{i}{2\pi}P\int_{-\infty}^{\infty} \frac{d\omega}{\omega} f'(\omega)$$

$$= -\frac{i}{2\pi\Delta}[f(\Delta) + f(-\Delta)]$$

$$+ \frac{i}{2\pi}\int_0^{\Delta} \frac{d\omega}{\omega}[f'(\omega) - f'(-\omega)]$$

$$- \frac{1}{2\pi}\int_0^{\infty} \frac{d\omega}{(i\omega + \Delta)^2}[f(\Delta + i\omega) + f(-\Delta - i\omega)]. \tag{48}$$

The numerical procedure was checked in several different ways. First, we evaluated all corrections in two gauges, the Feynman and the Coulomb one. The two calculations agree very well with each other. We found the direct and the exchange parts of the two-electron contribution and the three-electron correction to be separately gauge invariant on the level of the numerical accuracy. As an independent cross-check, we calculated directly the difference between the full QED contribution and the second-order MBPT result. To do this, we observe that the MBPT contribution can be obtained from the general QED formulas if we neglect the energy dependence of the photon propagator in the Coulomb gauge and introduce projection operators on the positive-energy part of the Dirac spectrum. So we evaluate the difference

TABLE I. Various contributions to the two-photon exchange correction for the 2s state of Li-like ions, in atomic units.

Z	$\Delta E^{2\mathrm{el}}(\mathrm{dir})$	$\Delta E^{2\mathrm{el}}(\mathrm{exch})$	$\Delta E^{3\mathrm{el}}$	Total
20	−0.16567	0.03293	−0.12545	−0.25819
30	−0.17053	0.03213	−0.12975	−0.26815
40	−0.17768	0.03104	−0.13605	−0.28269
50	−0.18759	0.02968	−0.14468	−0.30259
60	−0.20100	0.02811	−0.15614	−0.32903
70	−0.21904	0.02644	−0.17117	−0.36377
80	−0.24353	0.02484	−0.19097	−0.40966
83	−0.25254	0.02441	−0.19808	−0.42621
90	−0.27748	0.02361	−0.21736	−0.47123
92	−0.28582	0.02345	−0.22368	−0.48605
100	−0.32635	0.02332	−0.25356	−0.55659

TABLE III. Individual contributions to the two-photon exchange correction for the 2s and $2p_{1/2}$ states of Li-like Sn ($Z = 50$) in the Feynman and Coulomb gauges, in atomic units.

| | 2s | | $2p_{1/2}$ | |
	Feynman	Coulomb	Feynman	Coulomb
$\Delta E_{\mathrm{pole}}^{2\mathrm{el}}(\mathrm{dir})$	−0.18094	−0.18081	−0.30672	−0.30668
$\Delta E_{\mathrm{ir}}^{2\mathrm{el}}(\mathrm{dir})$	−0.00699	−0.00678	−0.01650	−0.01647
$\Delta E_{\mathrm{red}}^{2\mathrm{el}}(\mathrm{dir})$	0.00034	0.00000	0.00005	−0.00002
$\Delta E_{\mathrm{ir}}^{2\mathrm{el}}(\mathrm{exch})$	0.02648	0.02595	0.02200	0.02572
$\Delta E_{\mathrm{red}}^{2\mathrm{el}}(\mathrm{exch})$	0.00320	−0.00028	0.00328	−0.00043
$\Delta E_{\mathrm{ir}}^{3\mathrm{el}}$	−0.14574	−0.14461	−0.19718	−0.19454
$\Delta E_{\mathrm{red}}^{3\mathrm{el}}$	0.00106	−0.00007	0.00268	0.00005
Total	−0.30259	−0.30259	−0.49239	−0.49237

between the QED and the MBPT correction by performing the term-by-term subtraction first, and the ω integration after that. The MBPT contribution can be calculated separately up to very high accuracy after the ω integration is carried out analytically.

IV. NUMERICAL RESULTS AND DISCUSSION

Numerical results for the two-photon exchange correction, which corresponds to the interaction of the valence electron with the $(1s)^2$ shell in high-Z Li-like ions, are presented in Tables I and II for the 2s and $2p_{1/2}$ valence states, respectively. The total numerical uncertainty is estimated to be less than 3×10^{-5} a.u. for $Z=30–83$, less than 4×10^{-5} a.u. for $Z=20$, 90, and 92, and less than 5×10^{-5} a.u. for $Z=100$. In the tables, the two-photon exchange correction is divided into the direct, the exchange, and the three-electron parts. Each of these is found to be separately gauge invariant within the quoted error bars. The actual evaluation was carried out in two gauges, the Feynman and the Coulomb one. In Table III we present the individual contributions of the calculation for Li-like Sn ($Z = 50$) in these two gauges. In the table, $\Delta E_{\mathrm{ir}}^{2\mathrm{el}}(\mathrm{dir})$ denotes

TABLE II. Various contributions to the two-photon exchange correction for the $2p_{1/2}$ state of Li-like ions, in atomic units.

Z	$\Delta E^{2\mathrm{el}}(\mathrm{dir})$	$\Delta E^{2\mathrm{el}}(\mathrm{exch})$	$\Delta E^{3\mathrm{el}}$	Total
20	−0.77562	0.04211	0.34519	−0.38832
30	−0.45972	0.03838	0.01026	−0.41108
40	−0.35858	0.03286	−0.11926	−0.44498
50	−0.32316	0.02528	−0.19450	−0.49238
60	−0.31775	0.01516	−0.25444	−0.55703
70	−0.33168	0.00176	−0.31490	−0.64482
80	−0.36309	−0.01608	−0.38624	−0.76541
83	−0.37629	−0.02256	−0.41133	−0.81018
90	−0.41535	−0.04029	−0.47959	−0.93523
92	−0.42902	−0.04616	−0.50224	−0.97742
100	−0.49837	−0.07429	−0.61231	−1.18497

the direct part of the two-electron irreducible contribution originating from the integration over the imaginary axis, and $\Delta E_{\mathrm{pole}}^{2\mathrm{el}}(\mathrm{dir})$ is the corresponding pole contribution.

Our results can be compared with the latest evaluations by Andreev *et al.* [25] for $Z=30$, 70, 80, and 92, and by Sapirstein and Cheng [26] for $Z=83$. Fair agreement is observed in all cases except one, namely, the $2p_{1/2}$ state and $Z=70$. In that case, our calculation yields $−17.546(3)$ eV, compared to $−17.450(3)$ eV obtained in Ref. [25]. The reason for this discrepancy is not known at present.

Now we discuss the relation between our rigorous QED evaluation and traditional methods based on the treatment of the electron-electron interaction within the Breit approximation. Strictly speaking, the second-order (in $1/Z$) Breit approximation is valid up to order $(Z\alpha)^2$, and, therefore, *a priori* it is unclear whether it can be successfully applied for high-Z ions. The relativistic MBPT treatment is also based on the Breit approximation and, correspondingly, is valid up to order $(Z\alpha)^2$. However, it includes some higher-order terms also. Although one might think that keeping terms of order higher than $(Z\alpha)^2$ is excessive within this approximation, for atoms with one electron outside the $(1s)^2$ shell the MBPT treatment yields an approximation that is essentially better than the two first terms of the $Z\alpha$ expansion. To order $(Z\alpha)^2$ the two-photon exchange correction can be written as

$$\Delta E^{(2)} = E_{02} + (Z\alpha)^2(E_{22} + B_{22}), \qquad (49)$$

where $E_{02}(2s) = −0.250\,498$ and $E_{02}(2p_{1/2}) = −0.370\,911$ [27,28]; $E_{22}(2s) = −0.2427$, $B_{22}(2s) = −0.1129$, $E_{22}(2p_{1/2}) = −0.5265$, and $B_{22}(2p_{1/2}) = −0.2734$ [28].

Different approaches to the evaluation of the two-photon exchange correction are compared in Table IV and in Fig. 7. The second-order MBPT contribution can be divided into three parts corresponding to the exchange by two Coulomb photons (C), by one Coulomb and one Breit unretarded photon (B), and by two unretarded Breit photons $(B \times B)$. The most notable feature of our consideration is that effects neglected in the MBPT consideration are remarkably small in our case. For the $2p_{1/2}$-2s transition in Li-like uranium, the

TABLE IV. Comparison of rigorous QED calculations of the two-photon exchange correction for the $2p_{1/2}$-$2s$ transition in Li-like ions with the two first terms of the $Z\alpha$ expansion and with the second-order MBPT results. C denotes the second-order MBPT contribution due to the exchange of two Coulomb photons, B corresponds to the exchange of one Coulomb and one Breit photon, and $B \times B$ stands for the exchange of two Breit photons. Units are a.u.

Z	QED	$(Z\alpha)^0 + (Z\alpha)^2$	$C+B$	$C+B+(B \times B)$
20	−0.13013	−0.12988	−0.13012	−0.13011
30	−0.14293	−0.14171	−0.14300	−0.14298
40	−0.16229	−0.15827	−0.16246	−0.16245
50	−0.18979	−0.17956	−0.19017	−0.19029
60	−0.22800	−0.20559	−0.22870	−0.22913
70	−0.28105	−0.23635	−0.28211	−0.28322
80	−0.35575	−0.27183	−0.35710	−0.35946
83	−0.38397	−0.28340	−0.38536	−0.38825
90	−0.46400	−0.31206	−0.46539	−0.46990
92	−0.49137	−0.32067	−0.49268	−0.49778
100	−0.62838	−0.35701	−0.62919	−0.63731

extra physics contributes to about 1.3% if the $B \times B$ term is included into the MBPT treatment, and about 0.3% otherwise. A similar conclusion was drawn in Ref. [10] for non-degenerate excited states of He-like ions. This is in contrast to the ground-state case of He-like ions, where the difference of the QED and the MBPT results is on the level of 10% in the high-Z region [3]. Our comparison also shows that, while the $B \times B$ term is of the same order of magnitude as non-trivial QED contributions omitted in the MBPT approximation, adding this term makes the MBPT result deviate slightly more from the rigorous QED treatment.

Summarizing, we can conclude that in our case MBPT yields an approximation that is essentially better than the two first terms of the $Z\alpha$ expansion. This means that in an effective way MBPT can incorporate a certain part of the higher-order contributions. It is important to note, however, that some care should be taken in dividing results of the rigorous QED treatment into the MBPT part and the "beyond MBPT" part. The reason is that the MBPT contribution is not gauge invariant [it can be shown to be gauge invariant up to order $(Z\alpha)^2$ only], and it is often defined in different ways in the literature.

V. $2P_{1/2}$-$2S$ TRANSITION ENERGY IN Li-LIKE IONS

In Table V we collect all contributions calculated up to now for the $2p_{1/2}$-$2s$ transition energy in high-Z Li-like ions. The values of rms radii used in the calculation are taken from Refs. [29–33] and listed in the second column of the table. The splitting of the Dirac levels due to the finite nuclear size and the one-photon exchange correction are calculated using the Fermi model of the nuclear charge distribution,
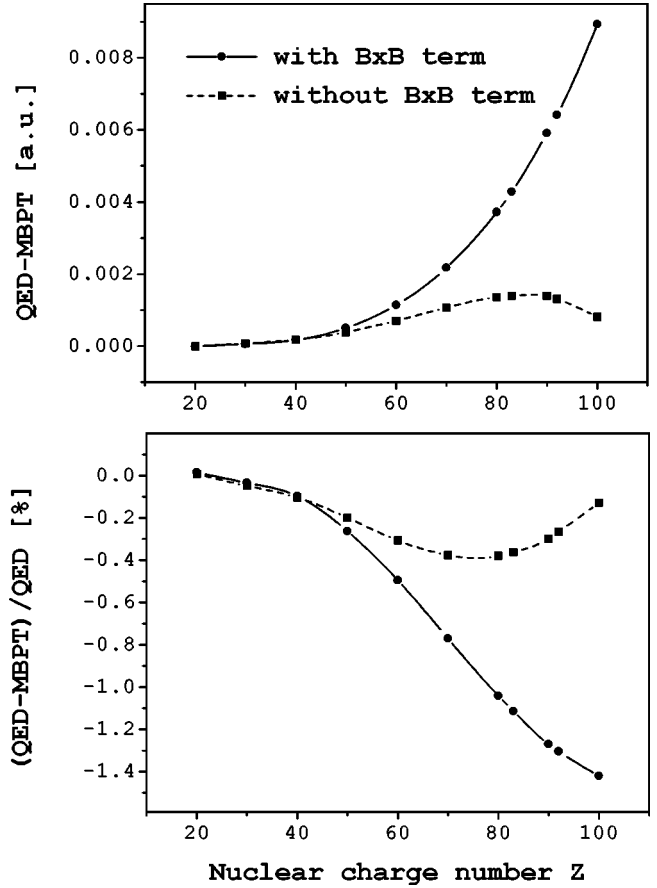
$$\rho(r) = \frac{N}{1 + \exp[(r-c)/a]}, \tag{50}$$

FIG. 7. Deviation of the rigorous QED treatment of the two-photon exchange correction for the $2p_{1/2}$-$2s$ transition energy in Li-like ions from the second-order MBPT results. The solid and the dashed lines correspond to the MBPT correction with and without the $B \times B$ term (the exchange by two Breit photons), respectively.

where the parameter a is fixed to be $a = 2.3/(4 \ln 3)$ fm. The parameters c and N are expressed in terms of the rms radius (see, e.g., Ref. [34]),

$$c^2 = \frac{5}{3}\langle r^2 \rangle - \frac{7}{3}a^2\pi^2, \tag{51}$$

$$N = \frac{3}{4\pi c^3}\left(1 + \frac{\pi^2 a^2}{c^2}\right)^{-1}. \tag{52}$$

The uncertainty of the nuclear-size effect was estimated by the 1% variation of the rms radius for all ions except Pb, Bi, Th, and U. For the latter ions, rms radii are known more precisely. Their errors are obtained by averaging available data and given in the second column of the table. The uncertainty of the nuclear-size effect in this case is estimated by varying the rms radii and by taking the difference between the correction calculated within the Fermi- and the spherical-distribution models with the same rms radius.

TABLE V. Individual contributions to the $2p_{1/2}$-$2s$ transition energy in Li-like ions. The first error ascribed to the total results originates from uncertainties of the individual contributions listed in the table. The second error arises from unknown one-electron α^2 QED effects and three-photon SE and VP screening corrections. Fin.nucl., finite nuclear size; 1ph, one-photon exchange; SE+VP, first-order self-energy and vacuum polarization; 2ph(MBPT), second-order MBPT; 2ph(QED), difference between the QED and the MBPT results for the two-photon exchange correction; 3ph, three-photon exchange; Scr.SE, screened self-energy; Scr.VP, screened vacuum polarization; Nucl.rec., nuclear recoil. Units are eV.

Element	$\langle r^2 \rangle^{1/2}$	Fin.nucl.	1ph	SE+VP	2ph(MBPT)	2ph(QED)	3ph	Scr.SE	Scr.VP	Nucl.rec.	Total
$^{40}_{18}$Ar	3.427	-0.001	35.570	-0.157	-3.489	0.000	$-0.075(3)$	0.028	-0.002	-0.010	31.865(3)(1)
$^{40}_{20}$Ca	3.478	-0.002	39.769	-0.226	-3.540	0.000	$-0.064(3)$	0.036	-0.002	-0.012	35.960(3)(2)
$^{58}_{28}$Ni	3.776	-0.010	57.455	-0.716	-3.807	0.000	$-0.034(4)$	0.084	-0.006	-0.015	52.951(4)(4)
$^{64}_{30}$Zn	3.928	-0.014	62.147	-0.906	-3.890	0.001	$-0.029(4)$	0.100	-0.008	-0.016	57.384(4)(4)
$^{74}_{32}$Ge	4.072	-0.021	66.967	-1.129	-3.981	0.001	$-0.023(5)$	0.117	-0.010	-0.016	61.906(5)(4)
$^{90}_{40}$Zr	4.270	-0.07	87.76	-2.41	-4.42	0.00	$-0.00(1)$	0.20	-0.02	-0.02	81.03(1)(1)
$^{107}_{47}$Ag	4.544	-0.18	108.43	-4.17	-4.92	0.01	$0.01(1)$	0.30	-0.03	-0.02	99.43(1)(1)
$^{120}_{50}$Sn	4.655	-0.27	118.17	-5.14	-5.18	0.01	$0.02(1)$	0.35	-0.04	-0.03	107.90(1)(2)
$^{132}_{54}$Xe	4.787	$-0.44(1)$	132.11	-6.69	-5.56	0.02	$0.03(1)$	0.43	-0.05	-0.03	119.82(2)(2)
$^{142}_{60}$Nd	4.914	$-0.89(2)$	155.44	-9.59	-6.24	0.03	$0.04(2)$	0.56	-0.07	-0.03	139.25(3)(4)
$^{164}_{66}$Dy	5.224	$-1.87(3)$	182.31	-13.32	-7.06	0.05	$0.06(3)$	0.71	-0.11	-0.03	160.74(4)(5)
$^{174}_{70}$Yb	5.317	$-2.92(5)$	202.61	-16.33	-7.71	0.06	$0.07(3)$	0.82	-0.13	-0.04	176.44(6)(7)
$^{184}_{74}$W	5.373	$-4.49(8)$	225.21	-19.83	-8.45	0.07	$0.08(4)$	0.94	-0.16	-0.04	193.33(9)(8)
$^{197}_{79}$Au	5.437	$-7.68(12)$	257.29(1)	-24.95	-9.54	0.10	$0.10(5)$	1.10	-0.20	-0.05	216.17(13)(11)
$^{202}_{80}$Hg	5.467	$-8.59(14)$	264.30(1)	-26.09	-9.78	0.10	$0.10(5)$	1.13	-0.21	-0.05	220.93(15)(11)
$^{208}_{82}$Pb	5.504(4)	$-10.67(2)$	278.99	-28.47	-10.29	0.11	$0.11(6)$	1.20	-0.24	-0.05	230.68(6)(13)
$^{209}_{83}$Bi	5.533(20)	$-11.94(7)$	286.68	-29.72	-10.56	0.12	$0.12(6)$	1.23	-0.25	-0.05	235.62(9)(13)
$^{232}_{90}$Th	5.802(4)	$-26.63(9)$	348.29	-39.68	-12.79	0.16	$0.16(7)$	1.46	-0.33	-0.07	270.60(11)(18)[a]
$^{238}_{92}$U	5.860(2)	$-33.35(7)$	368.83	-42.93	-13.55	0.17	$0.17(8)$	1.52	-0.36	-0.07	280.48(11)(20)[b]
$^{257}_{100}$Fm	5.886	$-79.0(1.0)$	468.63(3)	-57.88	-17.34	0.24	$0.24(12)$	1.68	-0.46	-0.11	316.0(1.0)(0.3)

[a]Includes 0.02 eV from nuclear polarization.
[b]Includes 0.03 eV from nuclear polarization.

The one-electron self-energy (SE) correction and the Wichman-Kroll part of the one-electron vacuum-polarization (VP) correction are taken from recent tabulations [35,36]. The Uehling part of the one-electron VP correction is calculated using the Fermi model of the nuclear charge distribution. Two-electron SE and VP corrections are taken from our previous evaluations [17,18]. The nuclear recoil correction was calculated by Artemyev *et al.* [37], and the nuclear-polarization correction for thorium and uranium was studied by Plunien *et al.* [38] and by Nefiodov *et al.* [39]. The total correction due to the two-photon exchange, evaluated in this work, is divided into two parts, the second-order MBPT contribution and the difference between the exact QED and the MBPT results. The MBPT contribution is obtained by neglecting the energy dependence of the photon propagator in the Coulomb gauge in the general formulas of Sec. II, and introducing projectors on the positive-energy part of the spectrum. It consists of the C, B, and $B \times B$ terms.

Corrections involving an exchange by three photons are suppressed roughly by a factor of $1/Z$ as compared to the two-photon contribution and, therefore, are small but not negligible. In Ref. [40] we evaluated the three-photon exchange correction within the Breit approximation, by taking the difference between the relativistic configuration-interaction result obtained with hydrogenlike wave functions

and the sum of the zeroth-, first-, and second-order (in $1/Z$) contributions calculated with the same hydrogenlike basis. In this work we reevaluate this correction with an increased number of configurations. It is worthwhile to note that the Breit interaction is responsible for the dominant part of the three-electron correction in the high-Z region. So the pure Coulomb part of the three-photon exchange contribution amounts to 0.04 eV for bismuth and 0.06 eV for uranium, while the total correction is about three times larger and contributes 0.12 eV and 0.17 eV, respectively. Taking into account the restricted nature of the Breit approximation, we ascribe the uncertainty of about 50% to the three-photon exchange correction in the high-Z region.

For the lowest values of Z considered here, the accuracy of our calculation of the three-photon exchange correction is not high enough. Taking into account that in this region the difference between the QED and the MBPT results for the two-photon exchange correction is negligible on the level of the total numerical accuracy, the data presented in the table for the three-photon exchange for $Z \leq 32$ were obtained from the MBPT calculations [45,46].

As the second-order one-electron QED corrections are not yet completely calculated, they are not included in the table. The recent status of these calculations has been discussed in Ref. [41]. The calculation of the last remaining correction of

TABLE VI. Comparison between theoretical calculations and experimental results for the $2p_{1/2}$-$2s$ transition energy in Li-like ions (in eV).

Z	This paper	Ref. [47]	Ref. [48]	Ref. [49]	Ref. [25]	Experiment	Reference
18	31.865(3)(1)	31.868(1)				31.866(1)	[50]
20	35.960(3)(2)	35.964(1)	35.963			35.962(2)	[51]
28	52.951(4)(4)					52.950(2)	[52]
						52.950(1)	[53]
						52.947(4)	[13]
30	57.384(4)(4)	57.389(2)			57.34(1)	57.384(3)	[13]
32	61.906(5)(4)	61.911(2)	61.907			61.902(4)	[52]
						61.901(2)	[54]
40	81.03(1)(1)	81.04					
47	99.43(1)(1)					99.438(7)	[14]
50	107.90(1)(2)	107.92(1)				107.911(8)	[15]
54	119.82(2)(2)	119.84(1)	119.82			119.97(10)	[55]
						119.820(8)	[15]
60	139.25(3)(4)	139.29(1)					
70	176.44(6)(7)	176.56(2)			176.52(10)		
74	193.33(9)(8)		193.33				
80	220.93(15)(11)	220.99(3)			220.92(20)		
82	230.68(6)(13)		230.70				
90	270.60(11)(18)	270.72(5)	270.69 [a]				
92	280.48(11)(20)	280.68(10)[a]	280.58 [a]	280.54(15)	280.36(21)	280.59(9)	[11]

[a]Corrected for the recent value of the nuclear-polarization effect [38,39].

order α^2, the two-loop self-energy, is still in progress [42–44]. Radiative corrections of order α^3 can be estimated as the two-photon SE and VP screening corrections suppressed by a factor of $1/Z$. Our rough estimate of the second-order one-electron and higher-order QED effects is represented by the second error ascribed to the total result in the table. The first error corresponds to the other sources of uncertainty, which are quoted in the table.

Table VI presents the comparison of the present evaluation of the $2p_{1/2}$-$2s$ transition energy in Li-like atoms with previous calculations and available experimental results. As compared to our previous compilation [17], in the present paper we reduce the total uncertainty of the predictions, due to the rigorously calculated effect of the two-photon exchange. Still, a direct calculation of the second-order one-electron QED contribution is desirable in order to ascribe a well-defined error to the theoretical predictions.

In summary, with this paper we conclude the series of our investigations on the two- and three-electron corrections of order α^2. We have evaluated all these contributions to the $2p_{1/2}$-$2s$ transition energy in Li-like high-Z ions. In this paper we presented a rigorous QED calculation of the two-photon exchange diagrams and an evaluation of the three-photon exchange correction within the Breit approximation. We collected all presently available contributions to the $2p_{1/2}$-$2s$ transition energy and compared the resulting predictions with the experimental results. While the total accuracy of the theoretical predictions is significantly improved, a

rigorous calculation of the second-order one-electron QED effects is still required.

APPENDIX

The summation over the magnetic substates in Eqs. (33)–(36) yields

$$F_{\text{lad,dir}}^{n_1 n_2}(\omega) = \alpha^2 \sum_{L_1 L_2} R_{L_1}(\omega, c v n_1 n_2) R_{L_2}(\omega, c v n_1 n_2)$$

$$\times \frac{(-1)^{L_1+L_2}}{2j_v+1} \sum_k (2k+1) \begin{Bmatrix} j_1 & L_2 & j_c \\ L_1 & j_2 & j_v \\ j_c & j_v & k \end{Bmatrix},$$

(A1)

$$F_{\text{lad,ex}}^{n_1 n_2}(\omega) = \alpha^2 \sum_{L_1 L_2} R_{L_1}(\omega, vcn_1 n_2) R_{L_2}(\omega - \Delta, cvn_1 n_2)$$

$$\times \frac{1}{2j_v + 1} \begin{Bmatrix} j_c & j_1 & L_1 \\ j_v & j_2 & L_2 \end{Bmatrix}, \qquad (\text{A2})$$

$$F_{\text{cr,dir}}^{n_1 n_2}(\omega) = \alpha^2 \sum_{L_1 L_2} R_{L_1}(\omega, cn_2 n_1 v) R_{L_2}(\omega, cn_2 n_1 v)$$

$$\times \frac{1}{2j_v + 1} \sum_k (2k+1) \begin{Bmatrix} j_1 & L_2 & j_c \\ L_1 & j_2 & j_v \\ j_c & j_v & k \end{Bmatrix}, \qquad (\text{A3})$$

$$F_{\text{cr,ex}}^{n_1 n_2}(\omega) = \alpha^2 \sum_{L_1 L_2} R_{L_1}(\omega, vn_2 n_1 v) R_{L_2}(\omega - \Delta, cn_2 n_1 c)$$

$$\times \frac{(-1)^{j_v - j_c}}{2j_v + 1} \sum_k (-1)^k (2k+1)$$

$$\times \begin{Bmatrix} j_1 & L_2 & j_c \\ L_1 & j_2 & j_v \\ j_v & j_c & k \end{Bmatrix}. \qquad (\text{A4})$$

The explicit expression for the radial integral $R_L(\omega, abcd)$ can be found in Ref. [17].

[1] R.E. Marrs, S.R. Elliott, and Th. Stöhlker, Phys. Rev. A **52**, 3577 (1995).

[2] Th. Stöhlker, S.R. Elliott, and R.E. Marrs, Hyperfine Interact. **99**, 217 (1996).

[3] S.A. Blundell, P.J. Mohr, W.R. Johnson, and J. Sapirstein, Phys. Rev. A **48**, 2615 (1993).

[4] I. Lindgren, H. Persson, S. Salomonson, and L.N. Labzowsky, Phys. Rev. A **51**, 1167 (1995).

[5] V.A. Yerokhin, A.N. Artemyev, and V.M. Shabaev, Phys. Lett. A **234**, 361 (1997).

[6] A.N. Artemyev, V.M. Shabaev, and V.A. Yerokhin, Phys. Rev. A **56**, 3529 (1997).

[7] H. Persson, S. Salomonson, P. Sunnergren, and I. Lindgren, Phys. Rev. Lett. **76**, 204 (1996).

[8] P. Sunnergren, Ph.D. thesis, Chalmers University of Technology, 1998.

[9] A.N. Artemyev, T. Beier, G. Plunien, V.M. Shabaev, G. Soff, and V.A. Yerokhin, Phys. Rev. A **62**, 022116 (2000).

[10] P.J. Mohr and J. Sapirstein, Phys. Rev. A **62**, 052501 (2000).

[11] J. Schweppe, A. Belkacem, L. Blumenfeld, N. Claytor, B. Feinberg, H. Gould, V.E. Kostroun, L. Levy, S. Misawa, J.R. Mowat, and M.H. Prior, Phys. Rev. Lett. **66**, 1434 (1991).

[12] P. Beiersdorfer, A.L. Osterheld, J.H. Scofield, J.R. Crespo López-Urrutia, and K. Widmann, Phys. Rev. Lett. **80**, 3022 (1998).

[13] U. Staude, Ph. Bosselmann, R. Büttner, D. Horn, K.-H. Schartner, F. Folkmann, A.E. Livingston, T. Ludziejewski, and P.H. Mokler, Phys. Rev. A **58**, 3516 (1998).

[14] Ph. Bosselmann, U. Staude, D. Horn, K.-H. Schartner, F. Folkmann, A.E. Livingston, and P.H. Mokler, Phys. Rev. A **59**, 1874 (1999).

[15] D. Feili, Ph. Bosselmann, K.-H. Schartner, F. Folkmann, A.E. Livingston, E. Träbert, X. Ma, and P.H. Mokler, Phys. Rev. A **62**, 022501 (2000).

[16] C. Brandau, Ph.D. thesis, University of Gießen, 2000.

[17] V.A. Yerokhin, A.N. Artemyev, T. Beier, G. Plunien, V.M. Shabaev, and G. Soff, Phys. Rev. A **60**, 3522 (1999).

[18] A.N. Artemyev, T. Beier, G. Plunien, V.M. Shabaev, G. Soff, and V.A. Yerokhin, Phys. Rev. A **60**, 45 (1999).

[19] V.A. Yerokhin, A.N. Artemyev, V.M. Shabaev, M.M. Sysak, O.M. Zherebtsov, and G. Soff, Phys. Rev. Lett. **85**, 4699 (2000).

[20] V.M. Shabaev, Sov. Phys. J. **33**, 660 (1990).

[21] V.M. Shabaev, Phys. Rev. A **50**, 4521 (1994).

[22] V.M. Shabaev, Phys. Rep. (to be published).

[23] V.M. Shabaev and I.G. Fokeeva, Phys. Rev. A **49**, 4489 (1994).

[24] W.R. Johnson, S.A. Blundell, and J. Sapirstein, Phys. Rev. A **37**, 307 (1988).

[25] O. Yu. Andreev, L.N. Labzowsky, G. Plunien, and G. Soff Phys. Rev. A (to be published).

[26] J. Sapirstein and K.T. Cheng, Phys. Rev. A **64**, 022502 (2001).

[27] U.I. Safronova and V.S. Senashenko, *Theory of Highly Ionized Spectra* (Energoatomizdat, Moscow, 1984) (in Russian).

[28] U.I. Safronova, W.R. Johnson, and M.S. Safronova, Phys. Scr. **58**, 348 (1998).

[29] G. Fricke, C. Bernhardt, K. Heilig, L.A. Schaller, L. Schellenberg, E.B. Shera, and C.W. de Jager, At. Data Nucl. Data Tables **60**, 177 (1995).

[30] H. de Vries, C.W. de Jager, and C. de Vries, At. Data Nucl. Data Tables **36**, 495 (1987).

[31] J.D. Zumbro, R.A. Naumann, M.V. Hoehn, W. Reuter, E.B. Shera, C.E. Bemis, Jr., and Y. Tanaka, Phys. Lett. **167B**, 383 (1986).

[32] J.D. Zumbro, E.B. Shera, Y. Tanaka, C.E. Bemis, Jr., R.A. Naumann, M.V. Hoehn, W. Reuter, R.M. Steffen, Phys. Rev. Lett. **53**, 1888 (1984).

[33] W.R. Johnson and G. Soff, At. Data Nucl. Data Tables **33**, 405 (1985).

[34] V.M. Shabaev, J. Phys. B **26**, 1103 (1993).

[35] T. Beier, P.J. Mohr, H. Persson, and G. Soff, Phys. Rev. A **58**, 954 (1998).

[36] T. Beier, G. Plunien, M. Greiner, and G. Soff, J. Phys. B **30**, 2761 (1998).

[37] A.N. Artemyev, V.M. Shabaev, and V.A. Yerokhin, Phys. Rev. A **52**, 1884 (1995).

[38] G. Plunien and G. Soff, Phys. Rev. A **51**, 1119 (1995); **53**, 4614 (1996).

[39] A.V. Nefiodov, L.N. Labzowsky, G. Plunien, and G. Soff, Phys. Lett. A **222**, 227 (1996).

[40] O.M. Zherebtsov, V.M. Shabaev, and V.A. Yerokhin, Phys. Lett. A **277**, 227 (2000).

[41] P.J. Mohr, G. Plunien, and G. Soff, Phys. Rep. **293**, 227 (1998).

[42] S. Mallampalli and J. Sapirstein, Phys. Rev. A **57**, 1548 (1998).

[43] I. Goidenko, L. Labzowsky, A. Nefiodov, G. Plunien, S. Zschocke, and G. Soff, Hyperfine Interact. **127**, 293 (2000).

[44] I. Goidenko, L. Labzowsky, A. Nefiodov, G. Plunien, S. Zschocke, and G. Soff, in *Hydrogen Atom: Precision Physics of Simple Atomic Systems*, edited by S. Karshenboim *et al.* (Springer, Berlin, in press).

[45] W.R. Johnson, S.A. Blundell, and J. Sapirstein, Phys. Rev. A **37**, 2764 (1988).

[46] Y.-K. Kim, D.H. Baik, P. Indelicato, and J.P. Desclaux, Phys. Rev. A **44**, 148 (1991).

[47] S. Blundell, Phys. Rev. A **47**, 1790 (1993).

[48] M.H. Chen, K.T. Cheng, W.R. Johnson, and J. Sapirstein, Phys. Rev. A **52**, 266 (1995).

[49] H. Persson, I. Lindgren, L.N. Labzowsky, G. Plunien, T. Beier, and G. Soff, Phys. Rev. A **54**, 2805 (1996).

[50] B. Edlén, Phys. Scr. **28**, 51 (1983).

[51] J. Sugar and C. Corliss, J. Phys. Chem. Ref. Data Suppl. **14**, 2 (1985).

[52] H. Hinnov and B. Denne, Phys. Rev. A **40**, 4357 (1989).

[53] J. Sugar, V. Kaufman, and W.L. Rowan, J. Opt. Soc. Am. B **9**, 344 (1992); **10**, 13 (1993).

[54] R.J. Knize, Phys. Rev. A **43**, 1637 (1991).

[55] S. Martin, J.P. Buchet, M.C. Buchet-Poulizac, A. Denis, J. Desesquelles, M. Druetta, J.P. Grandin, D. Hennecart, X. Husson, and D. Leclerc, Europhys. Lett. **10**, 645 (1989).